10342 *Biochemistry* **2009,** *48,* 10342–10352
DOI: 10.1021/bi900866s

BIOCHEMISTRY
including biophysical chemistry & molecular biology
Article

Molecular Characterization of Flubendiamide Sensitivity in the Lepidopterous Ryanodine Receptor Ca^{2+} Release Channel†

Kenta Kato,‡ Shigeki Kiyonaka,‡,§ Yuichi Sawaguchi,‡ Masanori Tohnishi,∥ Takao Masaki,∥ Noriaki Yasokawa,∥ Yusuke Mizuno,‡ Emiko Mori,‡ Keisuke Inoue,‡ Itaru Hamachi,‡,§ Hiroshi Takeshima,⊥ and Yasuo Mori*,‡,§

‡*Department of Synthetic Chemistry and Biological Chemistry, Graduate School of Engineering, Kyoto University, Kyoto 615-8510, Japan,* §*CREST, JST, Kyoto 615-8510, Japan,* ∥*Research Division, Nihon Nohyaku Company, Ltd., Osaka 586-0094, Japan, and* ⊥*Department of Biological Chemistry, Graduate School of Pharmaceutical Sciences, Kyoto University, Kyoto 606-8501, Japan*

Received May 21, 2009; Revised Manuscript Received August 29, 2009

ABSTRACT: Flubendiamide is a benzenedicarboxamide derivative that shows selective insecticidal activity against lepidopterous insects. The specific modulatory effects of flubendiamide on ryanodine binding in insect muscle microsomal membranes suggest that the ryanodine receptor (RyR) Ca^{2+} release channel is a primary target of flubendiamide. However, the molecular mechanisms underlying the species-specific action of flubendiamide are unclear. We have cloned cDNA encoding a novel RyR from the lepidopterous silkworm RyR (sRyR) and tested the sensitivity to flubendiamide of the recombinant sRyR in HEK293 cells. Confocal localization studies and Ca^{2+} imaging techniques revealed that sRyRs form Ca^{2+} release channels in the endoplasmic reticulum. Importantly, flubendiamide induced release of Ca^{2+} through the sRyR, but not through the rabbit RyR isoforms. Photoaffinity labeling of sRyR deletion mutants using a photoreactive derivative revealed that flubendiamide is mainly incorporated into the transmembrane domain (amino acids 4111−5084) of the sRyR. The rabbit cardiac muscle isoform RyR2 (rRyR2) and the RyR mutant carrying a replacement of the transmembrane domain (residues 4084−5084) with its counterpart sequence from rRyR2 (residues 3936−4968) were not labeled by the photoreactive compound. This replacement in the sRyR significantly impaired the responses to flubendiamide but only marginally reduced the sensitivity to caffeine, a general RyR activator. Furthermore, deletion of the N-terminal sequence (residues 183−290) abolished the responses of the sRyR to flubendiamide but not the sensitivity to caffeine. Our results suggest that the transmembrane domain plays an important role in the formation of an action site for flubendiamide, while the N-terminus is a structural requirement for flubendiamide-induced activation of the sRyR.

The ryanodine receptor (RyR)[1] is a large tetrameric channel that coordinates release of Ca^{2+} from the sarco/endoplasmic reticulum (SR/ER) to directly regulate Ca^{2+}-dependent cellular processes (*1*). The RyR consists of ∼5000 amino acids with a membrane-spanning domain at the C-terminal end and a hydrophilic domain at the N-terminal end. The C-terminal hydrophobic domain, which was predicted to contain 4−12 transmembrane segments, encompassing approximately one-fifth of the protein size, forms the pore of the Ca^{2+} release channel, while the large N-terminal cytoplasmic domain termed the "foot structure" spans the junctional gap between the transverse tubules and SR membranes (*2*, *3*). It has been proposed that the specific interaction between the cytoplasmic and transmembrane domains is an important mechanism in the intrinsic modulation of the RyR (*4*). Interestingly, defects in the intra-RyR interaction are likely to be responsible for aberrant Ca^{2+} release in RyR-linked pathology (*5*−*8*).

There are three isoforms of RyR proteins in mammals (*9*−*11*). RyR1 is the dominant isoform in skeletal muscle. RyR2 is found in high levels in cardiac muscle. RyR3 is expressed in many tissues, including the diaphragm and brain. They are similar in primary structure (∼66% identical sequences), except for three regions with high degrees of variability (*12*). RyRs serve critical roles, including excitation−contraction (EC) coupling in muscle cells. In skeletal muscle, the primary control of RyR1 occurs via an interaction with plasmalemmal dihydropyridine receptors (DHPRs), which function as voltage sensors for EC coupling and as L-type Ca^{2+} channels (*13*). In addition to "receiving" the EC coupling signal from the DHPR, RyR1 also "transmits" a retrograde signal that enhances the Ca^{2+} channel activity of the DHPR (*14*). Unlike RyR1, RyR2 can support Ca^{2+} entry-induced Ca^{2+} release, but neither mediates skeletal-type EC coupling or transmits the retrograde signal that enhances the Ca^{2+} channel activity of the skeletal DHPR (*15*).

The physiological importance of the RyR in insect muscle implies that basic understanding of EC coupling, which has been postulated from evidence presented in comprehensive investigations (*16*), is broadly deducible in the animal kingdom, including Class Insecta. The *Drosophila melanogaster* RyR or the *Caenorhabditis elegans* RyR is distinct equally from the mammalian subtypes in terms of primary structure (*17*), suggesting evolutionary divergence from one invertebrate subtype to the three

†This work was supported by grants from the Ministry of Education, Culture, Sports, Science and Technology of Japan.

*To whom correspondence should be addressed: Department of Synthetic Chemistry and Biological Chemistry, Graduate School of Engineering, Kyoto University, Nishikyo-ku, Kyoto 615-8510, Japan. Phone: +81-75-383-2761. Fax: +81-75-383-2765. E-mail: mori@sbchem.kyoto-u.ac.jp.

[1]Abbreviations: RyR, ryanodine receptor; SR, sarcoplasmic reticulum; ER, endoplasmic reticulum; EC, excitation−contraction; DHPR, dihydropyridine receptor; sRyR, silkworm RyR; WT, wild type; rRyR1, rabbit RyR1; rRyR2, rabbit RyR2; rRyR3, rabbit RyR3; DMEM, Dulbecco's modified Eagle's medium; $[Ca^{2+}]_i$, intracellular Ca^{2+} concentration; HBS, HEPES-buffered saline; SERCA, sarco/endoplasmic reticulum Ca^{2+}-ATPase.

 Published on Web 10/06/2009

functionally distinguishable vertebrate subtypes. The *Drosophila* RyR shares only 44−46% amino acid identity with the mammalian isoforms of the RyR (*18*). The regions with a high degree of structural divergence among the mammalian and insect isoforms of the RyR may serve as potential targets for potent insecticides that interact specifically with the insect but not mammalian isoforms. In muscle cells from different insect species, abundant receptor sites that are directly linked to the pore region of the Ca^{2+} release channel are present for ryanodine (*19*−*22*), a plant alkaloid that was originally used as an insecticide. However, ryanodine is also toxic to mammals and exerts a muscle-paralyzing effect in humans (*18*). Despite exploration of synthetic derivatives of the alkaloid and extensive structure−activity studies, ryanodol is the only widely recognized commercial product that targets RyRs via this approach (*20*, *23*). Rational design of a potent compound with high species specificity requires an extensive understanding of the function and regulation of the RyR present in insect cells and extensive structural information.

Recently, two classes of benzenedicarboxamides have emerged as novel insecticides that target insect RyRs: the phthalic diamides, including flubendiamide, and the anthranilic diamides, including chloranthraniliprole. These diamides have potent insecticidal activity; phthalic and anthranilic diamides were reported to elicit intracellular Ca^{2+} release in isolated *Heliothis* neurons (*24*, *25*) and in *Periplaneta americana* neurons (*26*), respectively. Binding studies on microsomal membranes from insect muscles suggest that flubendiamide and chlorantraniliprole interact with a site distinct from the ryanodine binding site on the insect RyR complex (*25*, *26*). Characteristic symptoms such as body contraction, feeding cessation, and paralysis caused by flubendiamide are similar to those caused by chlorantraniliprole. The action of flubendiamide is highly specific, with selective toxicity in restricted insect taxa, including *Lepidoptera* (*24*). This is in contrast to chlorantraniliprole, which induces Ca^{2+} responses not only in lepidopterous insects but also in mammals at concentrations exceeding 10 μM (*27*). Thus, flubendiamide, in addition to chlorantraniliprole, is a new experimental tool for exploring the physiological effects of RyR activity, even though the exact binding sites for flubendiamide or chlorantraniliprole have not yet been identified. Furthermore, the molecular mechanisms underlying the differences in species selectivity between flubendiamide and chlorantraniliprole are not yet understood.

To study the species-specific agonist activity of flubendiamide, we isolated cDNA encoding the RyR from the lepidopterous silkworm (sRyR) and established the functional expression of the recombinant sRyR to characterize the site of action of flubendiamide. The results suggest that flubendiamide induces release of Ca^{2+} through the sRyR by acting on the transmembrane domain, and the flubendiamide response of sRyR requires the N-terminal cytoplasmic domain. Our findings provide important information for understanding the species-selective effects of RyR activators.

EXPERIMENTAL PROCEDURES

Materials. Caffeine was obtained from Wako, ryanodine from alomone laboratories, fura-2 AM ester from Dojindo, and Mag-fura-2 AM ester from Biotium. Flubendiamide and *N*-(4-chloro-2-methyl-6-{[(1-methylethyl)amino]carbonyl}phenyl)-1-(3-chloro-2-pyridinyl)-3-(trifluoromethyl)-1*H*-pyrazole-5-carboxamide (DP-23) were synthesized as previously reported (*24*, *28*). A flubendiamide-based trifunctional photoaffinity probe (flubendiamide-PP) was synthesized. For details, see Scheme 1 of the Supporting Information.

cDNA Cloning and Construction of Expression Vectors. The genomic DNA sequence encoding the sRyR was identified by a computer search of homologues of the cDNA sequence encoding the *Drosophila* RyR (GenBank accession number D17389) through a silkworm genomic DNA shotgun sequence using KAIKOBLAST (*29*). RT-PCR and cDNA library screening were used to amplify the entire coding sequence of the sRyR cDNA from silkworm RNA isolated from muscle, using forward and reverse primers designed on the basis of the genomic DNA sequence of the sRyR. Consequently, six overlapping cDNA fragments were obtained and sequenced. The entire coding sequence of sRyR is registered as GenBank accession number DJ085056. sRyR cDNA was subcloned into the pCI-neo vector (Promega). In the deletion mutants Δ183−290, Δ183−1065, Δ183−2233, and Δ183−4110, nucleotides 547−870, 547−3195, 547−6699, and 547−12330 of the sRyR cDNA, respectively, were deleted. The wild-type (WT) sRyR, Δ183−290, Δ183−1065, Δ183−2233, and Δ183−4110 were fused at the N-terminus with EGFP using PCR techniques. The cDNAs encoding rabbit RyR1 (rRyR1) and rabbit RyR2 (rRyR2) were cloned into eukaryotic expression vectors pRRS11 and pHRRS1, respectively (*9*, *10*). The 14.8 kb *Xho*I (vector)−*Xho*I (vector) fragment of pNRR42 carrying the entire protein coding sequence of rabbit RyR3 (rRyR3) (*11*) was subcloned into the pCI-neo vector. In construct s-r2, the cytosolic region of the sRyR (amino acids 1−4083) was substituted in-frame for the corresponding rRyR2 sequence (amino acids 1−3935). The cDNA encoding s-r2 was subcloned into pCI-neo vector and pEGFP vector (Clontech).

Cell Culture and cDNA Expression in HEK293 Cells. HEK293 cells were cultured in Dulbecco's modified Eagle's medium (DMEM) containing 10% fetal bovine serum, 30 units/mL penicillin, and 30 μg/mL streptomycin (*30*). Transfection of cDNA plasmids was conducted using SuperFect Transfection Reagent according to the manufacturer's instructions (Qiagen). The cells were subjected to Western blotting, confocal imaging, measurement of changes in intracellular Ca^{2+} concentration ($[Ca^{2+}]_i$) or luminal Ca^{2+} concentration, and photoaffinity labeling 32−52 h after transfection.

Western Blotting. Forty-eight hours after transfection, HEK293 cells were solubilized in RIPA buffer (pH 8.0) containing 0.1% sodium dodecyl sulfate, 0.5% sodium deoxycholate, 1% Nonided P40, 150 mM NaCl, 50 mM Tris-HCl, 1 mM PMSF, and 10 μg/mL leupeptin and then centrifuged at 17400*g* for 20 min. The cell lysates were fractionated via 5% sodium dodecyl sulfate−polyacrylamide gel electrophoresis (SDS−PAGE) and electrotransferred onto a nitrocellulose membrane (Pall Corp.) or a polyvinylidene fluoride membrane (Pall Corp.). The blots were incubated with an anti-EGFP antibody (Clontech) and stained using the SuperSignal system (Thermo Fisher).

Confocal Imaging. Thirty-two hours after transfection, HEK293 cells were plated onto poly-L-lysine-coated glass base dishes (IWAKI). Four to six hours after the cells had been plated on the coverslips, fluorescence images were acquired with a confocal laser scanning microscope (Olympus FV500) using the 488 nm line of an argon laser for excitation and a 505 to 525 nm band-pass filter for emission (EGFP) or the 543 nm line of a HeNe laser for excitation and a 560 nm long-pass filter for emission (DsRed monomer). The specimens were viewed at high

magnification using plan oil objectives (60×, 1.40 numerical aperture, Olympus).

Measurement of Changes in $[Ca^{2+}]_i$. The fura-2 fluorescence was measured in HEPES-buffered saline (HBS) containing 107 mM NaCl, 6 mM KCl, 1.2 mM $MgSO_4$, 2 mM $CaCl_2$, 1.2 mM KH_2PO_4, 11.5 mM glucose, and 20 mM HEPES (pH 7.4, adjusted with NaOH) in HEK293 cells. The 340 nm:380 nm ratio images were converted to Ca^{2+} concentrations by in vivo calibration using 5 μM ionomycin (Calbiochem) (*30*). All the reagents dissolved in water or dimethyl sulfoxide (DMSO) were diluted to their final concentrations in HBS or Ca^{2+}-free HBS containing 107 mM NaCl, 6 mM KCl, 1.2 mM $MgSO_4$, 0.5 mM EGTA, 1.2 mM KH_2PO_4, 11.5 mM glucose, and 20 mM HEPES (pH 7.4, adjusted with NaOH) and applied to the cells by perfusion. EC_{50} values were determined by using KaleidaGraph (Synergy Software).

Measurement of Changes in the Luminal Ca^{2+} *Concentration*. Cells were attached to poly-L-lysine-coated coverslips and loaded with Mag-fura-2 by incubation in DMEM containing 10 μM Mag-fura-2 AM ester and 10% fetal bovine serum, 30 units/mL penicillin, and 30 μg/mL streptomycin at 37 °C. The Mag-fura-2-loaded cells were then permeabilized by being incubated in 100 μM β-escin (Sigma) for 2−5 min in an internal solution containing 19 mM NaCl, 125 mM KCl, 10 mM HEPES, 1.4 mM $MgCl_2$, 0.66 mM $CaCl_2$, and 1 mM EGTA (pH 7.3, adjusted with KOH) to wash out Mag-fura-2 in the cytoplasm, which enabled measurement of the Ca^{2+} concentration within the organelles (*31*). The specific β-escin exposure time was empirically determined in each experiment by monitoring the loss of Mag-fura-2 fluorescence from cytoplasm and nucleus (*32*). The ratio of fluorescence intensities by excitations at 340 and 380 nm of 10−14 cells within a frame was normalized so that 1 and 0 corresponded to the values just before the test application of flubendiamide and after the depletion of the store following application of 100 μM flubendiamide, respectively. The initial 20 s period for the normalized time course was fitted with a single-exponential function, e^{-rt}. The rate constant, r (s^{-1}), thus estimated was used as an index of the RyR activity.

Photoaffinity Labeling. EGFP-sRyR (WT)-, EGFP-sRyR (Δ183−290)-, EGFP-sRyR (Δ183−1065)-, EGFP-sRyR (Δ183−2233)-, EGFP-sRyR (Δ183−4110)-, EGFP-s-r2-, or rRyR2-expressing HEK293 cells (~6×10^6) were treated with flubendiamide-PP (100 or 30 μM) and Pluronic F-127 (0.1%) (Sigma) in HBS, and photolabeling was conducted by UV light irradiation (365 nm) at room temperature (22−25 °C) for 1 h. The cells were collected and washed three times with PBS at 7700*g* for 10 s at 4 °C and then lysed by a freeze−thaw cycle in RIPA buffer (pH 8.0) containing 0.1% SDS, 0.5% sodium deoxycholate, 1% Nonided P40, 150 mM NaCl, 50 mM Tris-HCl, 0.1 mM PMSF, 0.50 μg/mL leupeptin, 0.50 μg/mL aprotinin, 0.60 μg/mL pepstatin A, 0.75 mM benzamizine, 2.0 μM calpain I inhibitor, and 2.0 μM calpeptin. Flubendiamide-PP-bound proteins were pulled down from the cell lysates with a 70 μL bed volume of Immobilized NeutrAvidin Protein Plus (Pierce) at 4 °C for 4−12 h. The beads were washed with RIPA buffer, and proteins were eluted in SDS sample buffer. The proteins were analyzed by 5% SDS−PAGE and Western blotting with an anti-EGFP antibody or anti-RyR2 antibody (Affinity BioReagents).

Statistical Analysis. All data are expressed as means ± the standard error of the mean (SEM). The data were accumulated under each condition from at least three independent experiments. The *P* values are the results of Student's *t* tests.

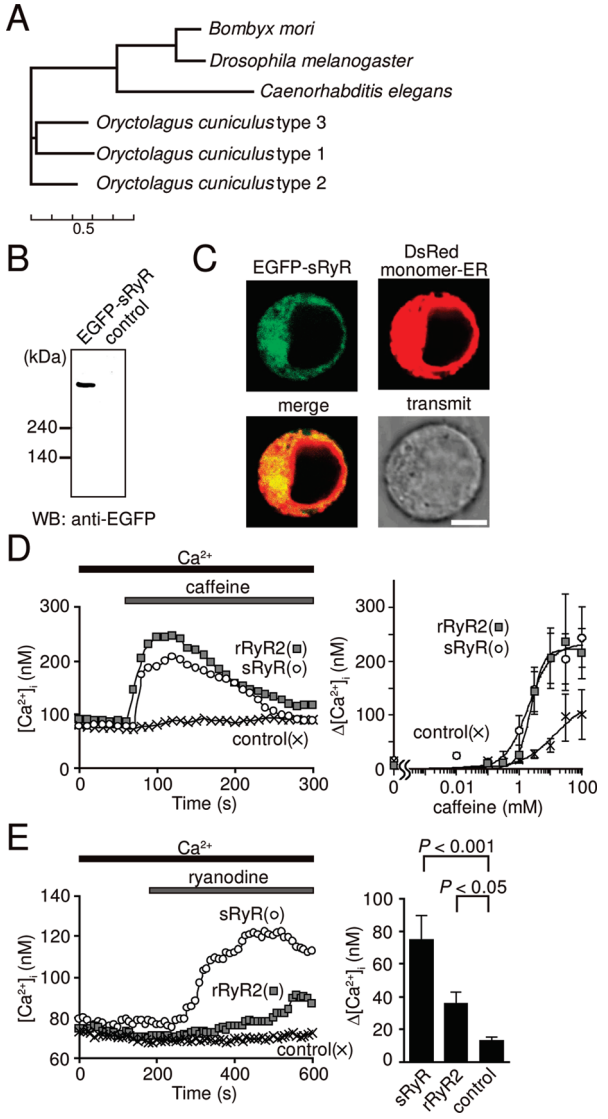

FIGURE 1: Functional expression of the sRyR in HEK293 cells. (A) Amino acid phylogram of RyRs constructed using ClustalW version 1.83. (B) Western blotting (WB) of recombinant expression of the EGFP-sRyR in HEK293 cell lysates using an anti-EGFP antibody. (C) Confocal imaging of the EGFP-sRyR and DsRed monomer ER recombinantly expressed in a HEK293 cell. The scale bar is 5 μm. (D) Caffeine-induced $[Ca^{2+}]_i$ increases in sRyR (○)-, rRyR2 (■)-, or control vector (×)-transfected HEK293 cells. Average time courses of Ca^{2+} responses induced by 10 mM caffeine (left). Concentration dependence of maximum $[Ca^{2+}]_i$ increases ($\Delta[Ca^{2+}]_i$) induced by caffeine (right) (n = 11−43). (E) Ryanodine-induced $[Ca^{2+}]_i$ increases in sRyR (○)- or rRyR2 (■)-expressing cells or in control vector (×)-transfected cells. Average time courses of Ca^{2+} responses (left) and maximum $[Ca^{2+}]_i$ increases (right) induced by 20 μM ryanodine (n = 49−116).

RESULTS

cDNA Cloning of the Silkworm Ryanodine Receptor. The genomic DNA sequence encoding the lepidopterous silkworm (*Bombyx mori*) RyR was identified by a computer search of homologues of the *Drosophila* cDNA sequence through the silkworm genomic DNA shotgun sequence. RT-PCR and cDNA library screening were used to amplify the entire coding sequence of the novel sRyR cDNA from silkworm RNA isolated from muscle. The entire protein of 5084 amino acids was deduced from the sRyR cDNA sequence. The amino acid phylogram shows that the invertebrate RyRs are grouped separately from the vertebrate isoforms (Figure 1A). The sRyR is highly identical

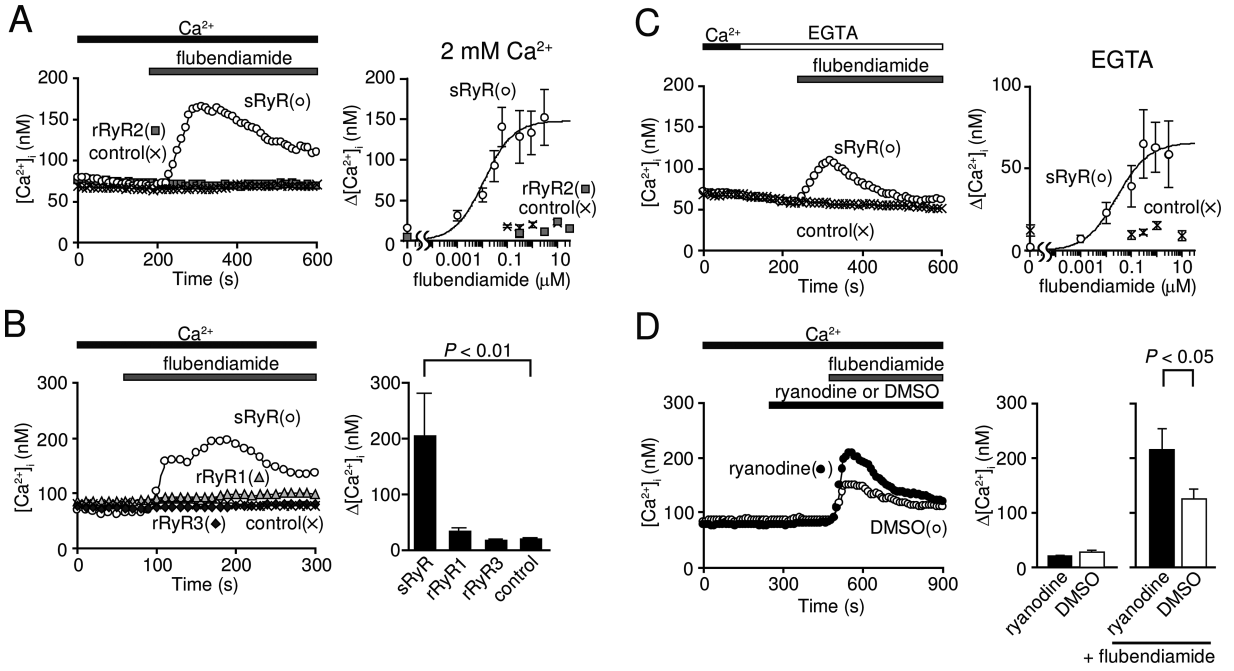

FIGURE 2: Flubendiamide selectively induces $[Ca^{2+}]_i$ increases in sRyR-expressing HEK293 cells. (A) $[Ca^{2+}]_i$ increases induced by flubendiamide in HEK293 cells transfected with the sRyR (○), but not in HEK293 cells transfected with rRyR2 (■) or the control vector (×) in a 2 mM Ca^{2+}-containing external solution. Average time courses of Ca^{2+} responses induced by 300 nM flubendiamide (left). Concentration dependence of maximum flubendiamide-induced $[Ca^{2+}]_i$ increases (right) (n = 23−106). (B) $[Ca^{2+}]_i$ increases induced by flubendiamide in HEK293 cells transfected with the sRyR (○), but not in HEK293 cells transfected with rRyR1 (▲), rRyR3 (◆), or the control vector (×) in a 2 mM Ca^{2+}-containing external solution. Average time courses of Ca^{2+} responses (left) and maximum $[Ca^{2+}]_i$ increases (right) induced by 30 μM flubendiamide (n = 11−20). (C) $[Ca^{2+}]_i$ increases induced by flubendiamide in HEK293 cells transfected with the sRyR (○), but not in HEK293 cells transfected with the control vector (×) in a Ca^{2+}-free, 0.5 mM EGTA-containing external solution. Average time courses of Ca^{2+} responses induced by 300 nM flubendiamide (left). Concentration dependence of maximum flubendiamide-induced $[Ca^{2+}]_i$ increases (right) (n = 25−82). (D) Cooperative activation of the sRyR by ryanodine and flubendiamide. After 1 μM ryanodine (●) or 0.01% DMSO (○) is applied to sRyR-transfected HEK293 cells for 4 min, 300 nM flubendiamide is added to the extracellular solution. Average time courses of Ca^{2+} responses (left). DMSO is used to dissolve ryanodine. Maximum $[Ca^{2+}]_i$ increases induced by ryanodine or DMSO prior to the addition of flubendiamide (middle). Maximum $[Ca^{2+}]_i$ increases induced by flubendiamide with ryanodine or DMSO (right) (n = 31 or 60, respectively).

with the *Drosophila* RyR (79%) but less identical with rabbit (*Oryctolagus cuniculus*) RyRs (45−47%).

Functional Expression and ER Localization of the sRyR in HEK293 Cells. The sRyR was heterologously expressed in HEK293 cells for investigation of the direct action of flubendiamide, because HEK293 cells should provide a simpler environment for comparing functional properties and dynamics of Ca^{2+} release of different isoforms of RyRs expressed under the same cellular context, in a manner independent of the variable number of muscle-specific accessory proteins. In fact, HEK293 cells do not endogenously express the accessory proteins or other physiological modulators of RyRs such as triadin, calsequestrin, and L-type Ca^{2+} channels (*33*−*36*). Western blotting using the construct tagged at the N-terminal end with EGFP confirmed the expression of the sRyR in HEK293 cells (Figure 1B). Confocal image analysis of the EGFP-sRyR revealed subcellular localization comparable with that of the DsRed monomer ER, which selectively targets the ER (Figure 1C) (*37*, *38*).

To examine the functional expression of sRyR, we conducted fluorescence imaging of $[Ca^{2+}]_i$ using the Ca^{2+} indicator fura-2. Caffeine induced $[Ca^{2+}]_i$ increases in HEK293 cells transfected with rRyR2 (Figure 1D), rRyR1, or rRyR3 (Figure 1 of the Supporting Information), as previously reported (*39*, *40*). The rRyR2 response was dose-dependent with an EC_{50} value of 2.7 ± 0.1 mM. Caffeine also dose-dependently induced $[Ca^{2+}]_i$ increases with an EC_{50} value of 2.2 ± 0.3 mM in HEK293 cells transfected with the sRyR, indicating functional expression of the sRyR in HEK293 cells. HEK293 cells transfected with the control vector also showed $[Ca^{2+}]_i$ increases in response to caffeine only at high concentrations. Expression of endogenous RyRs has been reported in HEK293 cells (*41*, *42*). RT-PCR analysis showed endogenous expression of RyR1 and RyR2 in HEK293 cells (Figure 2 of the Supporting Information), in accordance with a previous report (*41*). Endogenous RyRs may be involved in $[Ca^{2+}]_i$ increases induced by high concentrations of caffeine. Ryanodine (20 μM) also induced $[Ca^{2+}]_i$ increases in HEK293 cells expressing the sRyR or rRyR2 (Figure 1E). In agreement with our observation, it has been previously reported that the addition of ryanodine caused a slow release of Ca^{2+} in HEK293 cells expressing RyR2 (*43*).

Flubendiamide Selectively Induces Release of Ca^{2+} through the sRyR. Application of flubendiamide induced $[Ca^{2+}]_i$ increases in a 2 mM Ca^{2+}-containing external solution in a dose-dependent manner, with an EC_{50} value of 17 ± 4 nM in sRyR-expressing HEK293 cells, but failed to induce $[Ca^{2+}]_i$ increases in rRyR2-, rRyR1-, or rRyR3-expressing HEK293 cells, even at a higher concentration (30 μM) (Figure 2A,B). The EC_{50} value is comparable to the previously reported K_d value (4.7 nM) for binding of flubendiamide to *Heliothis* microsomal membranes (*25*). Flubendiamide also induced $[Ca^{2+}]_i$ increases in a 0.5 mM EGTA-containing Ca^{2+}-free external solution with a similar EC_{50} value (~20 nM) in sRyR-expressing cells (Figure 2C), indicating that flubendiamide induces release of Ca^{2+} via the sRyR from intracellular Ca^{2+} stores. Ryanodine alone at 1 μM failed to induce sRyR-mediated $[Ca^{2+}]_i$ increases, while preapplication and subsequent coapplication of 1 μM

ryanodine enhanced flubendiamide-induced $[Ca^{2+}]_i$ increases (Figure 2D). This is consistent with the idea that the sRyR responsible for the flubendiamide-induced $[Ca^{2+}]_i$ increases is, in fact, ryanodine-sensitive, further suggesting that flubendiamide and ryanodine cooperatively activate the sRyR.

We examined roles of calmodulin (CaM) and FK506-binding protein 12 (FKBP12), which modulate RyR channels (*44*), to determine the involvement of endogenous CaM and FKBP12 present in HEK293 cells (*45*, *46*). W7, a CaM inhibitor previously reported to reduce the amplitude of the caffeine-induced Ca^{2+} release (*47*, *48*), inhibited caffeine- or flubendiamide-induced $[Ca^{2+}]_i$ increases in sRyR-transfected HEK293 cells (Figure 3A, B of the Supporting Information), suggesting positive regulation of sRyR by CaM. However, flubendiamide is unlikely to act primarily through CaM, since RyR2, which is susceptible to regulation by CaM (*49*), does not respond to flubendiamide, when recombinantly expressed in HEK293 cells (Figure 2A). The FKBP12-binding motif carrying the valine-proline dipeptide epitope [amino acids 2450−2468 (ALRIRAILRSLVPLDDLVG)] identified in RyR1 (*50*, *51*) is conserved in the sRyR [amino acids 2519−2537 (SLRARAILRSLVPLEDLQG)]. FK506, which dissociates FKBP12 from RyR1 and RyR3 proteins to enhance caffeine-induced Ca^{2+} release via RyR1 and RyR3 (*52*−*55*), enhanced caffeine-induced $[Ca^{2+}]_i$ increases but failed to affect flubendiamide-induced $[Ca^{2+}]_i$ increases (Figure 3C,D of the Supporting Informaton), indicating that FKBP acts on the sRyR but does not influence the activation of the sRyR by flubendiamide.

Masaki et al. reported that flubendiamide stimulates the Ca^{2+} pump activity of sarco/endoplasmic reticulum Ca^{2+}-ATPase (SERCA) in a muscle membrane preparation from *Spodoptera litura* more extensively than the classical RyR modulators ryanodine and caffeine (*56*). Therefore, we tested whether flubendiamide also stimulates uptake of Ca^{2+} by SERCA that suppresses $[Ca^{2+}]_i$ increases. The cells were first exposed to 10 μM cyclopiazonic acid (CPA), a reversible inhibitor of SERCA, to deplete the Ca^{2+} stores in the absence of external Ca^{2+} (Figure 4 of the Supporting Informaton). The increase in $[Ca^{2+}]_i$ elicited by the subsequent addition of Ca^{2+} and washout of CPA was significantly smaller in silkworm SERCA (sSERCA)-expressing HEK293 cells than in control cells, but flubendiamide failed to affect this reduction, which is indicative of uptake of Ca^{2+} by SERCA. These results suggest that flubendiamide acts on the sRyR to induce Ca^{2+} release.

Direct assessment of Ca^{2+} release via the sRyR by monitoring the Ca^{2+} concentration in the lumen of Ca^{2+} stores using Mag-fura-2 (*31*, *32*) revealed that caffeine significantly reduced the luminal level of Ca^{2+} in sRyR- or rRyR2-expressing cells compared with control cells (Figure 3A), and flubendiamide significantly reduced the luminal level of Ca^{2+} in sRyR-expressing cells compared with rRyR2-expressing cells or control cells (Figure 3B) in a dose-dependent manner (Figure 3B,C). The dose−response curve of flubendiamide obtained in the luminal Ca^{2+} monitoring experiment showed an EC_{50} of ~400 nM, which is moderately higher than that obtained by cytoplasmic Ca^{2+} monitoring. The quantitative difference may arise from the use of Mag-fura-2 with a different sensitivity to Ca^{2+} or a difference in cellular configuration, which may affect the involvement of accessory components, or low concentrations of molecular factors necessary for the activation of the sRyR (see Discussion for further details). Interestingly, comparison with the store capacity determined using ionomycin, which fully

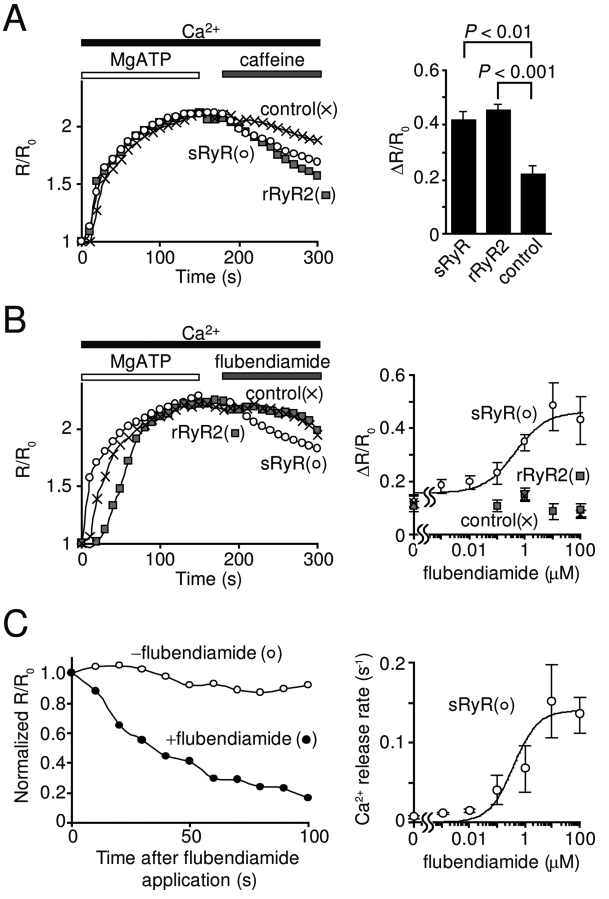

FIGURE 3: Flubendiamide induces release of Ca^{2+} through the sRyR. (A and B) The ER luminal Ca^{2+} concentration is increased with activation of the Ca^{2+} pump in the presence of MgATP and is decreased upon application of caffeine (A) or flubendiamide (B). The ratio (R) between intensities of the fluorescence at 340 and 380 nm excitation is divided by the initial ratio (R_0) to yield R/R_0. (A) Average time courses (left) and maximum decreases (right) of R/R_0 induced by 10 mM caffeine in HEK293 cells transfected with sRyR (○), rRyR2 (■), or the control vector (×) (n = 11−34). (B) Average time courses of R/R_0 induced by 1 μM flubendiamide in HEK293 cells transfected with sRyR (○), rRyR2 (■), or the control vector (×) (left). Concentration dependence of maximum decreases induced by flubendiamide (right) (n = 12−37). (C) Concentration dependence of release of Ca^{2+} through the sRyR induced by flubendiamide. Average time courses of normalized R/R_0 induced by 10 μM flubendiamide (●) or in the absence of flubendiamide (○) in HEK293 cells transfected with the sRyR (left) (see Experimental Procedures for normalization of R/R_0). Release rates were obtained by fitting the initial part of the Ca^{2+} decay signal to a single exponential (right) (n = 10−14).

depletes internal Ca^{2+} stores, revealed that release of Ca^{2+} induced by caffeine or flubendiamide at a concentration capable of inducing maximal responses (10 mM or 100 nM, respectively) (Figures 1D and 2A) was only from a fraction of stored Ca^{2+} (Figure 5 of the Supporting Informaton). This may also contribute to the discrepancy (see Discussion for further details). Thus, the sRyR channel is very likely to carry an action site for flubendiamide.

Direct Action of Flubendiamide on the sRyR. Photoaffinity labeling is a powerful tool for identifying target proteins of biologically active molecules. Multifunctional photoaffinity probes with a ligand moiety and a biotin tag have been used for cross-linking studies of ligand−receptor complexes (*57*−*59*). We conducted photoaffinity labeling using a flubendiamide-based trifunctional photoaffinity probe, flubendiamide-PP,

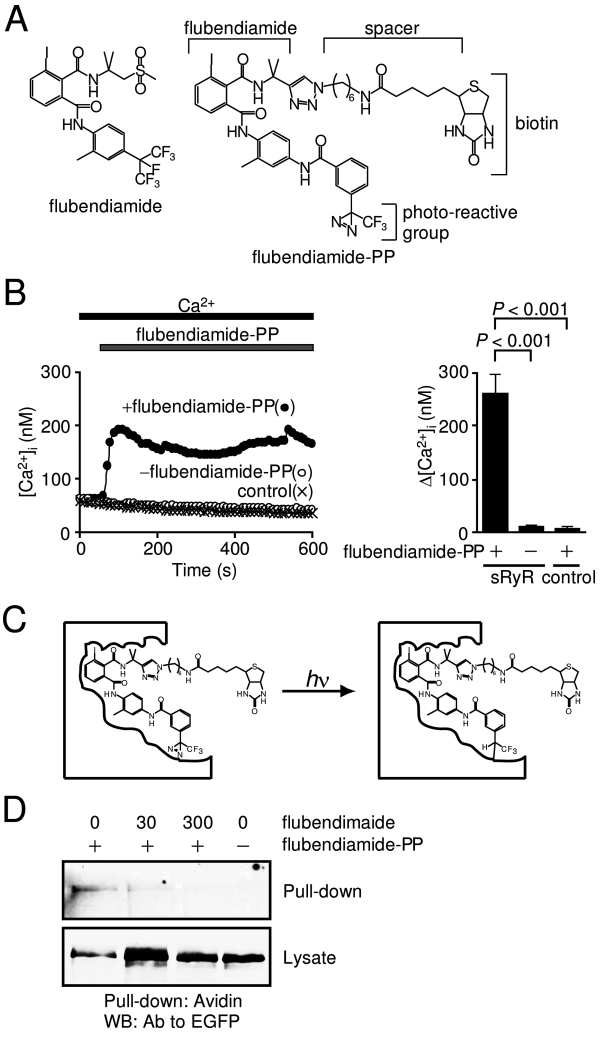

FIGURE 4: Photoaffinity labeling of the sRyR with flubendiamide-PP. (A) Chemical structures of flubendiamide (left) and flubendiamide-PP (right). (B) $[Ca^{2+}]_i$ increases induced by 100 μM flubendiamide-PP in HEK293 cells transfected with sRyR (●), but not in HEK293 cells transfected with the control vector (×). For flubendiamide-PP being loaded into cells, 0.1% Pluronic F127 that can permeabilize cells is added. F127 alone fails to induce $[Ca^{2+}]_i$ increases in HEK293 cells transfected with the sRyR (○). Average time courses of Ca^{2+} responses (left) and maximum $[Ca^{2+}]_i$ increases (right) induced by flubendiamide-PP (n = 29–49). (C) Schematic representation of the photoaffinity labeling method using flubendiamide-PP. The photoreaction forms a covalent bond between the ligand and target proteins, and biotin allows collections of labeled proteins using biotin–avidin binding. (D) Flubendiamide-PP directly binds the sRyR. After photochemical cross-linking with 100 μM flubendiamide-PP, EGFP-sRyR proteins are detected with an anti-EGFP antibody by WB in avidin pulled-down samples. The photochemical flubendiamide-PP cross-linking of the sRyR is inhibited by a 10 min preincubation and subsequent co-incubation with flubendiamide (30 or 300 μM).

which carries a biotin tag, a photoreactive group for subsequent covalent labeling, and a flubendiamide moiety, which targets the RyR (Figure 4A). Importantly, flubendiamide-PP retained the capacity to activate sRyR-mediated Ca^{2+} release (Figure 4B). In cells expressing the EGFP-sRyR (575 kDa) after photoirradiation in the presence of flubendiamide-PP, Western blotting using anti-EGFP antibodies revealed a band with a molecular mass greater than that of the 240 kDa marker, which corresponds well with the band in whole cell lysates from EGFP-sRyR-expressing cells (Figure 4C,D). The incorporation of flubendiamide-PP into this protein band was abolished by preincubation and subsequent co-incubation with flubendiamide in photoirradiation. Thus, flubendiamide is most likely incorporated directly into the sRyR.

The Transmembrane Domain of the sRyR Is Essential for Flubendiamide Binding. As indicated in Figure 5A, the well-known RyR domains, such as RyR, Spla and RyR (SPRY) (*60*), RyR and inositol 1,4,5-trisphosphate receptor (IP_3R) homology (RIH), RIH-associated (RIH assoc), and protein mannosyltransferase, IP_3R, and RyR (MIR) (*61*, *62*) are conserved in the sRyR. To identify regions in the sRyR that are essential for flubendiamide binding, we constructed four EGFP-fused deletion mutants of the sRyR, EGFP-sRyR (Δ183–290), EGFP-sRyR (Δ183–1065), EGFP-sRyR (Δ183–2233), and EGFP-sRyR (Δ183–4110). Δ183–4110 is a homologue of the RyR1 mutant, which lacks the amino acid residues from position 183 to 4006 but forms a functional Ca^{2+} release channel in the lipid bilayer membrane (*3*). sRyR mutants Δ183–290, Δ183–1065, and Δ183–2233 have deletions in the regions that correspond to the first 305, 1072, and 2150 N-terminal amino acids, respectively, of mouse RyR2, following the first 182 N-terminal residues of the sRyR. Mutants Δ183–290, Δ183–2233, and Δ183–4110 were present in the ER, like EGFP-sRyR (WT) in HEK293 cells, whereas mutant Δ183–1065 not only was present in ER but also exhibited cytoplasmic localization (Figure 6 of the Supporting Information). Western blotting revealed that the deletion mutants were expressed at levels comparable to that of WT (Figure 5B, left, bottom panel). For mutant Δ183–1065, we observed a pronounced high-molecular mass protein band, corresponding to the calculated molecular mass, and a lower-molecular mass band (Figure 5B, left, arrowhead), which may represent a degradation product of Δ183–1065. All of the deletion mutant proteins were photoaffinity-labeled by incubation with flubendiamide-PP (Figure 5B, left, top panel). In Δ183–1065, the lower-molecular mass band was found after photoirradiation in the absence of flubendiamide-PP, which is most likely due to nonspecific binding of avidin. Importantly, the incorporation of flubendiamide-PP into Δ183–4110 was abolished by preincubation and subsequent co-incubation with flubendiamide in photoirradiation (Figure 5B, right). These results suggest that the direct binding site for flubendiamide is formed by the transmembrane domain and/or the first 182-amino acid N-terminal sequence in the sRyR.

To confirm the indispensability of the transmembrane sequence of sRyR for flubendiamide binding, the sRyR mutant, s-r2, carrying a replacement of the transmembrane domain (amino acids 4084–5084) with its counterpart sequence from rRyR2 (amino acids 3936–4968) was constructed (Figure 5A). s-r2 and rRyR2 failed to exhibit photoaffinity labeling with flubendiamide-PP in contrast to sRyR (WT) (Figure 5C). These results suggest that the transmembrane domain is necessary but the first 182-amino acid N-terminal sequence alone is not sufficient for the formation of the flubendiamide binding site in the sRyR.

The Cytoplasmic Region (*amino acids 183–290*) *Is Required for the Intact Sensitivity of sRyR to Flubendiamide*. The functional effects of these mutations on the flubendiamide sensitivity of the sRyR channel were assessed by measuring the Ca^{2+} responses in HEK293 cells. It was previously reported that the first 305 N-terminal amino acids are not essential for caffeine-induced activation of RyR2, but deletion of the first 1072 or 2150 N-terminal amino acids abolishes

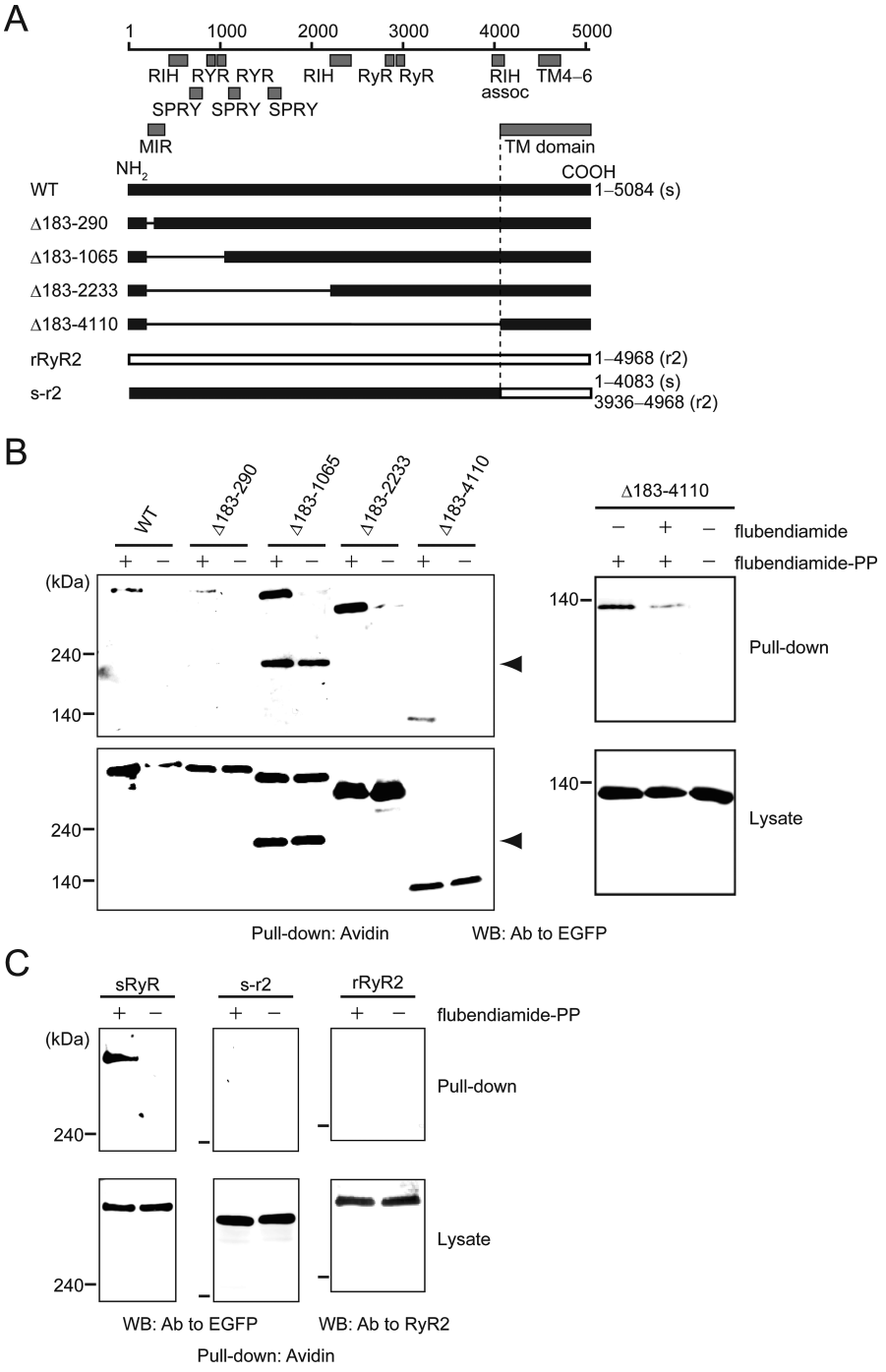

FIGURE 5: Transmembrane domain of sRyR that is sufficient for flubendiamide binding. (A) WT, deletion mutants of the sRyR, rRyR2, and s-r2 are depicted with deleted residues at the left. Domains homologous to RyR, SPRY, RIH, RIH assoc, MIR, and transmembrane region 4−6 of the RyR1 family (TM4−6) are indicated at the top for the sRyR. (B) Flubendiamide-PP is directly incorporated into the transmembrane domain of the sRyR. In the left panel, EGFP-sRyR (WT)-, EGFP-sRyR (Δ183−290)-, EGFP-sRyR (Δ183−1065)-, EGFP-sRyR (Δ183−2233)-, or EGFP-sRyR (Δ183−4110)-expressing HEK293 cells were treated with flubendiamide-PP. After being photochemically cross-linked with 30 μM flubendiamide-PP, EGFP-sRyR proteins were detected with an anti-EGFP antibody by WB in avidin pulled-down samples and lysates. In the right panel, the photochemical cross-linking with 30 μM flubendiamide-PP of EGFP-sRyR (Δ183−4110) is inhibited by a 10 min preincubation and subsequent co-incubation with flubendiamide (30 μM). (C) Photoaffinity labeling fails to incorporate flubendiamide-PP, which efficiently labels the sRyR, in s-r2 as well as rRyR2. After being photochemically cross-linked, EGFP-sRyR (WT), EGFP-s-r2, or rRyR2 proteins were subjected to WB with an anti-EGFP antibody or anti-RyR2 antibody in avidin pulled-down samples.

caffeine-induced activation of RyR2 in HEK293 cells (*51*). In fact, Δ183−1065, Δ183−2233, and Δ183−4110 significantly reduced the level of caffeine- and flubendiamide-induced Ca^{2+} release in HEK293 cells (Figure 6 A,B), suggesting that these deletions impair channel function. Interestingly, Δ183−290 showed $[Ca^{2+}]_i$ responses to caffeine (10 mM) but not to flubendiamide (30 μM) (Figure 6A,B). This result suggests the N-terminal sequence of residues 183−290 is a structural requirement for flubendiamide-induced activation in the sRyR.

The Transmembrane Domain Is Required for Intact Sensitivity of the sRyR to Flubendiamide. s-r2 showed significant Ca^{2+} release in response to caffeine comparable to that observed for the sRyR (Figure 6C), whereas it showed very little Ca^{2+} release in response to flubendiamide at 100 μM only

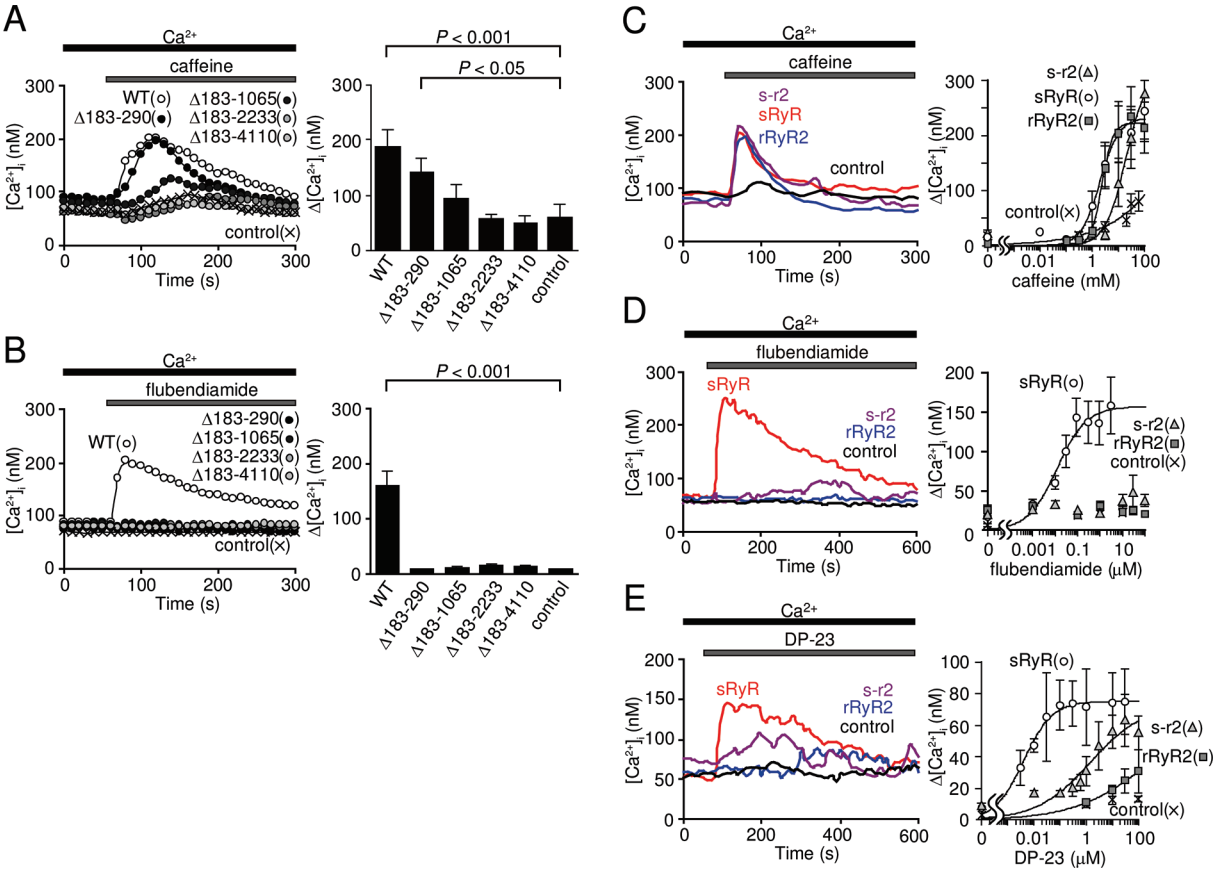

FIGURE 6: Sensitivity of the sRyR to flubendiamide that is abolished by the deletion of cytoplasmic sequence (residues 183−290) or the replacement of the transmembrane region with the counterpart of rRyR2. (A) Caffeine-induced $[Ca^{2+}]_i$ increases in HEK293 cells expressing deletion mutants of the EGFP-sRyR. Average time courses of Ca^{2+} responses (left) and maximum $[Ca^{2+}]_i$ increases (right) induced by 10 mM caffeine (n = 54−84). (B) Flubendiamide fails to induce responses of deletion mutants of the EGFP-sRyR. Average time courses of Ca^{2+} responses (left) and maximum $[Ca^{2+}]_i$ increases (right) induced by 30 μM flubendiamide (n = 11−36). (C) Caffeine induces nearly intact responses of s-r2 in HEK293 cells. Representative time courses of Ca^{2+} responses induced by 30 mM caffeine (left). Concentration dependence of maximum $[Ca^{2+}]_i$ increases induced by caffeine (n = 16−35) (right). (D) Flubendiamide response impaired in s-r2. Representative time courses of Ca^{2+} responses induced by 10 μM flubendiamide (left). Concentration dependence of maximum $[Ca^{2+}]_i$ increases induced by flubendiamide (n = 12−48) (right). (E) s-r2 shows a partially suppressed response to DP-23. Representative time courses of Ca^{2+} responses induced by 10 μM DP-23 (left). Concentration dependence of maximum $[Ca^{2+}]_i$ increases induced by DP-23 (right).

(Figure 6D), suggesting that the Ca^{2+} release channel activity is intact but its sensitivity to flubendiamide is disrupted in s-r2. We tested DP-23 (*28*) (see the chemical structure in Figure 7 of the Supporting Information), whose structural analogue chlorantraniliprole is known to exhibit ~300-fold greater selectivity toward the insect RyR, relative to the mammalian RyR (*27*). The DP-23-induced Ca^{2+} release activity of the sRyR was significantly higher than that of s-r2 and rRyR2 (Figure 6E), indicating that the second class of benzenedicarboxamide agonists, anthranilic diamides, also requires the transmembrane domain of the sRyR for intact activation. Interestingly, in contrast to flubendiamide, DP-23 induced significantly greater Ca^{2+} responses at concentrations of 0.01−30 μM in s-r2-expressing cells in comparison with those in rRyR2-expressing cells. This suggests that the transmembrane amino acid residues specific for the sRyR are more critical for flubendiamide sensitivity than DP-23 sensitivity, leading to the idea that the relative importance of the sRyR transmembrane domain is increased due to the selectivity of activators for the sRyR.

DISCUSSION

This study has demonstrated the structural basis for the sensitivity of sRyR channel activation to flubendiamide, a benzenedicarboxamide derivative. Flubendiamide is incorporated into the transmembrane domain (amino acids 4111−5084) of the sRyR (Figure 5B,C). s-r2, the sRyR construct comprised of the cytoplasmic foot domain (amino acids 1−4083) attached to the rRyR2 transmembrane domain (amino acids 3936−4968), fails to incorporate flubendiamide-PP and does not respond to flubendiamide, although it retains nearly intact sensitivity to caffeine (Figures 5C and 6C,D). Mutant Δ183−290, which lacks the N-terminal sequence (amino acids 183−290), has a binding site for flubendiamide-PP but does not respond to flubendiamide despite retaining sensitivity to caffeine (Figures 5B and 6A,B). Therefore, the sRyR also requires the N-terminus for flubendiamide sensitivity.

Flubendiamide induced $[Ca^{2+}]_i$ increases in the presence or absence of extracellular Ca^{2+} in sRyR-expressing cells (Figure 2A,C) but failed to induce $[Ca^{2+}]_i$ increases in rRyR1-, rRyR2-, or rRyR3-expressing cells (Figure 2A,B), which is consistent with the previously reported selective insecticidal activity of flubendiamide against lepidopterous pests (*24*). The dose−response curve of flubendiamide obtained in the luminal Ca^{2+} monitoring experiment is not completely consistent with that of $[Ca^{2+}]_i$ monitoring (Figures 2A and 3B). The difference between the two monitoring systems may arise from the loss of

key effectors important for the activation of the sRyR by the permeabilization procedure in luminal Ca^{2+} monitoring. In fact, RyR channels are complex structures modulated by regulatory or associated proteins such as CaM and FKBP (*44*). The inhibition of endogenous CaM by W7 (*47*, *48*) suppressed caffeine- or flubendiamide-induced $[Ca^{2+}]_i$ increases in sRyR-transfected HEK293 cells (Figure 3A,B of the Supporting Information), suggesting that CaM positively regulates the sRyR. FK506 enhanced caffeine-induced $[Ca^{2+}]_i$ increases but failed to affect flubendiamide-induced $[Ca^{2+}]_i$ increases (Figure 3C,D of the Supporting Information), indicating that FKBP does not influence the activation of the sRyR by flubendiamide. These results support the idea that the discrepancy may arise from the loss of CaM from cytoplasm in luminal Ca^{2+} monitoring. With regard to roles played by muscle-specific accessory proteins, it may be interesting to compare the function of the expressed sRyR in dyspedic myotubes (*14*, *63*−*65*), which express full sets of these proteins, with that in HEK293 cells. It is also possible that the discrepancy may arise from the difference in Ca^{2+} sensitivity of Mag-fura-2 and fura-2. The K_d values of Mag-fura-2 and fura-2 for Ca^{2+} binding are 53 and 0.22 μM, respectively (*66*, *67*), suggesting that upon limited release of Ca^{2+} by flubendiamide at low concentrations, the submicromolar decrease in the luminal Ca^{2+} concentration cannot be detected using Mag-fura-2, whereas the submicromolar increases in $[Ca^{2+}]_i$ are detected using fura-2. Interestingly, our experiment comparing Ca^{2+} release with the store capacity (Figure 5 of the Supporting Information) reveals that only a fraction of the Mag-fura-2-containing subcellular area is responsive to flubendiamide, suggesting that Mag-fura-2 can be present also in internal Ca^{2+} stores or organelles resistant to β-escin permeabilization and insensitive to flubendiamide. This raises an additional basis for the idea that we cannot detect small decreases in Ca^{2+} concentration elicited by low concentrations of flubendiamide in Ca^{2+} stores, for the case in which flubendiamide induces changes in Ca^{2+} concentrations around the saturated levels of the dynamic range of the Mag-fura-2 sensor.

The photoaffinity labeling compound flubendiamide-PP was incorporated into the WT sRyR and deletion mutant Δ183−4110, but not into rRyR2 or s-r2 (Figure 5B,C). s-r2 exhibited nearly intact responses to caffeine but only marginal responses to flubendiamide (Figure 6C,D), suggesting that binding to the transmembrane domain (amino acids 4111−5084) is critical for the intact response to flubendiamide in the sRyR. This is supported by the finding that s-r2 exhibited a sensitivity to DP-23 that was significantly lower than that of the sRyR (Figure 6E). Furthermore, N-terminal deletion mutant Δ183−290 exhibited responses to caffeine but not to flubendiamide, although it carries the binding site for flubendiamide (Figures 5B and 6A,B), indicating that amino acid residues 183−290 are essential for flubendiamide sensitivity in the sRyR. The N-terminal sequence of residues 183−290 is similar in primary structure to part of the IP_3/ryanodine receptor domain (amino acids 12−201 in the sRyR), which corresponds to the ligand binding region of the IP_3R (*68*), and also overlaps with the MIR domain (amino acids 212−393 in the sRyR), which may have a ligand transferase function (*61*, *62*). Collectively, these findings indicate that the N-terminal sequence plays an important role in sRyR activation in response to flubendiamide binding. Interestingly, it has been previously reported that the RyR1 construct RyR-C, which lacks amino acids 183−4006, forms a cation-selective channel that shares some of the channel properties of WT RyR1, including activation by cytoplasmic Ca^{2+} and regulation by ryanodine (*3*). However, unlike WT RyR1, which exhibits a linear current−voltage relationship and is inactivated at millimolar concentrations of Ca^{2+}, the channels formed by RyR-C display aberrant inward rectification and fail to close at high cytoplasmic Ca^{2+} concentrations (*3*). These results suggest that the C-terminal region of RyR1 contains structures sufficient to form a functional Ca^{2+} release channel, but the N-terminal region of RyR1 also affects ion conduction and calcium-dependent regulation of the Ca^{2+} release channel (*3*).

In malignant hyperthermia (MH)-susceptible patients, three mutation clusters have been identified in the RyR1 gene: the N-terminal region (amino acids 35−614), the central region (amino acids 2129−2458), and the C-terminal region (amino acids 3916−4942). Central core disease (CCD) has been linked to mutations in the RyR1 gene in the same regions of the RyR1 proteins as MH (*69*). Furthermore, missense mutations in cardiac RyR2 have been linked with catecholaminergic polymorphic ventricular tachycardia and a form of arrhythmogenic right ventricular dysplasia (*70*). Analogous to the MH/CCD mutations in RyR1, the RyR2 mutations cluster in three regions: in the N-terminus (amino acids 176−420), the central region (amino acids 2246−2504), and the C-terminal region (amino acids 3778−4950) which carries the transmembrane pore region (*70*, *71*). These genetic findings also support the importance of the N-terminal region and the C-terminal transmembrane domain for the normal function of RyRs. Intriguingly, in the sRyR, counterparts of the N-terminal and C-terminal regions of RyR1 and RyR2 overlap with the regions critical for flubendiamide sensitivity. Therefore, flubendiamide may exert agonistic effects on the sRyR through the N-terminal and C-terminal regions that are critical for the physiological function of the sRyR, by contrast with caffeine, which does not require the N-terminal region to activate the sRyR.

RyRs require an interaction between the cytoplasmic domain and the transmembrane domain to conduct Ca^{2+} (*4*, *72*). Activation of the RyR channel is associated with conformational reorganization of the cytoplasmic N-terminal structure and rotation of the C-terminal transmembrane assembly (*6*, *73*, *74*). George et al. proposed that amino acid residues 3722−4610 of the human RyR2 C-terminus (corresponding to amino acids 3870−4733 of sRyR) constitute an interacting domain that is involved in Ca^{2+} channel regulation, and that this interacting domain mediates the intramolecular but not intermolecular protein−protein interactions of RyR2 subunits in the intact tetramer (*4*). Our data strongly suggest that flubendiamide is incorporated into the transmembrane sequence of the sRyR (amino acids 4111−5084), which may contain the interacting domain. Callaway et al. proposed that ryanodine binds with high affinity to the proposed pore region in the C-terminal transmembrane domain of RyR1 (amino acids 4475−5037, corresponding to amino acids 4575−5084 of sRyR) (*22*). Furthermore, Ebbinghaus-Kintscher et al. reported that ryanodine does not interfere with flubendiamide binding (*25*). Taken together, these reports suggest that flubendiamide interacts with a binding site that is distinct from the ryanodine binding site localized in the pore of the RyR and acts cooperatively with ryanodine to activate the sRyR. Flubendiamide may regulate the conformational coupling between the cytoplasmic domain and the transmembrane domain by binding to the interacting domain. It is of interest to compare the effect of benzenedicarboxamide compounds on the sRyR with that of imperatoxin A, which activates mammalian RyRs at

nanomolar concentrations (*75*−*77*). To clarify the mechanisms by which flubendiamide binding promotes channel activation, a more detailed determination of the binding site and structural analysis using single-particle analysis with cryo-electron microscopy are needed.

SUPPORTING INFORMATION AVAILABLE

Supplemental experimental procedures, supplemental references, synthetic schemes of flubendiamide-PP and Figures 1−7. This material is available free of charge via the Internet at http://pubs.acs.org.

REFERENCES

1. Berridge, M. J., Lipp, P., and Bootman, M. D. (2000) The versatility and universality of calcium signalling. *Nat. Rev. Mol. Cell Biol. 1*, 11–21.
2. Takeshima, H. (1993) Primary structure and expression from cDNAs of the ryanodine receptor. *Ann. N.Y. Acad. Sci. 707*, 165–177.
3. Bhat, M. B., Zhao, J., Takeshima, H., and Ma, J. (1997) Functional calcium release channel formed by the carboxyl-terminal portion of ryanodine receptor. *Biophys. J. 73*, 1329–1336.
4. George, C. H., Jundi, H., Thomas, N. L., Scoote, M., Walters, N., Williams, A. J., and Lai, F. A. (2004) Ryanodine receptor regulation by intramolecular interaction between cytoplasmic and transmembrane domains. *Mol. Biol. Cell 15*, 2627–2638.
5. Zorzato, F., Menegazzi, P., Treves, S., and Ronjat, M. (1996) Role of malignant hyperthermia domain in the regulation of Ca^{2+} release channel (ryanodine receptor) of skeletal muscle sarcoplasmic reticulum. *J. Biol. Chem. 271*, 22759–22763.
6. El-Hayek, R., Saiki, Y., Yamamoto, T., and Ikemoto, N. (1999) A postulated role of the near amino-terminal domain of the ryanodine receptor in the regulation of the sarcoplasmic reticulum Ca^{2+} channel. *J. Biol. Chem. 274*, 33341–33347.
7. Yamamoto, T., El-Hayek, R., and Ikemoto, N. (2000) Postulated role of interdomain interaction within the ryanodine receptor in Ca^{2+} channel regulation. *J. Biol. Chem. 275*, 11618–11625.
8. Yamamoto, T., and Ikemoto, N. (2002) Peptide probe study of the critical regulatory domain of the cardiac ryanodine receptor. *Biochem. Biophys. Res. Commun. 291*, 1102–1108.
9. Takeshima, H., Nishimura, S., Matsumoto, T., Ishida, H., Kangawa, K., Minamino, N., Matsuo, H., Ueda, M., Hanaoka, M., Hirose, T., and Numa, S. (1989) Primary structure and expression from complementary DNA of skeletal muscle ryanodine receptor. *Nature 339*, 439–445.
10. Nakai, J., Imagawa, T., Hakamata, Y., Shigekawa, M., Takeshima, H., and Numa, S. (1990) Primary structure and functional expression from cDNA of the cardiac ryanodine receptor/calcium release channel. *FEBS Lett. 271*, 169–177.
11. Hakamata, Y., Nakai, J., Takeshima, H., and Imoto, K. (1992) Primary structure and distribution of a novel ryanodine receptor/calcium release channel from rabbit brain. *FEBS Lett. 312*, 229–235.
12. Sorrentino, V., and Volpe, P. (1993) Ryanodine receptors: How many, where and why? *Trends Pharmacol. Sci. 14*, 98–103.
13. Rios, E., and Brum, G. (1987) Involvement of dihydropyridine receptors in excitation-contraction coupling in skeletal muscle. *Nature 325*, 717–720.
14. Nakai, J., Dirksen, R. T., Nguyen, H. T., Pessah, I. N., Beam, K. G., and Allen, P. D. (1996) Enhanced dihydropyridine receptor channel activity in the presence of ryanodine receptor. *Nature 380*, 72–75.
15. Nakai, J., Ogura, T., Protasi, F., Franzini-Armstrong, C., Allen, P., and Beam, K. G. (1997) Functional nonequality of the cardiac and skeletal ryanodine receptors. *Proc. Natl. Acad. Sci. U.S.A. 94*, 1019–1022.
16. Takekura, H., and Franzini-Armstrong, C. (2002) The structure of Ca^{2+} release units in arthropod body muscle indicates an indirect mechanism for excitation-contraction coupling. *Biophys. J. 83*, 2742–2753.
17. Sakube, Y., Ando, H., and Kagawa, H. (1997) An abnormal ketamine response in mutants defective in the ryanodine receptor gene ryr-1(unc-68) of *Caenorhabditis elegans*. *J. Mol. Biol. 267*, 849–864.
18. Xu, X., Bhat, M. B., Nishi, M., Takeshima, H., and Ma, J. (2000) Molecular cloning of cDNA encoding a *Drosophila* ryanodine receptor and functional studies of the carboxyl-terminal calcium release channel. *Biophys. J. 78*, 1270–1281.
19. Schmitt, M., Turberg, A., and Londershausen, M. (1997) Characterization of a ryanodine receptor in *Periplaneta americana*. *J. Recept. Signal Transduction Res. 17*, 185–197.
20. Waterhouse, A. L., Pessah, I. N., Francini, A. O., and Casida, J. E. (1987) Structural aspects of ryanodine action and selectivity. *J. Med. Chem. 30*, 710–716.
21. Witcher, D. R., McPherson, P. S., Kahl, S. D., Lewis, T., Bentley, P., Mullinnix, M. J., Windass, J. D., and Campbell, K. P. (1994) Photoaffinity labeling of the ryanodine receptor/Ca^{2+} release channel with an azido derivative of ryanodine. *J. Biol. Chem. 269*, 13076–13079.
22. Callaway, C., Seryshev, A., Wang, J. P., Slavik, K. J., Needleman, D. H., Cantu, C., III, Wu, Y., Jayaraman, T., Marks, A. R., and Hamilton, S. L. (1994) Localization of the high and low affinity [^{3}H]ryanodine binding sites on the skeletal muscle Ca^{2+} release channel. *J. Biol. Chem. 269*, 15876–15884.
23. Lehmberg, E., and Casida, J. E. (1994) Similarity of insect and mammalian ryanodine binding sites. *Pestic. Biochem. Physiol. 48*, 145–152.
24. Tohnishi, M., Nakao, H., Furuyam, T., Seo, A., Kodama, H., Tsubata, K., Fujioka, S., Kodama, H., Hirooka, T., and Nishimatsu, T. (2005) Flubendiamide, a novel insecticide highly active against lepidopterous insect pests. *J. Pestic. Sci. 30*, 354–360.
25. Ebbinghaus-Kintscher, U., Luemmen, P., Lobitz, N., Schulte, T., Funke, C., Fischer, R., Masaki, T., Yasokawa, N., and Tohnishi, M. (2006) Phthalic acid diamides activate ryanodine-sensitive Ca^{2+} release channels in insects. *Cell Calcium 39*, 21–33.
26. Cordova, D., Benner, E. A., Sacher, M. D., Rauh, J. J., Sopa, J. S., Lahm, G. P., Selby, T. P., Stevenson, T. M., Flexner, L., Gutteridge, S., Rhoades, D. F., Wu, L., Smith, R. M., and Tao, Y. (2006) Anthranilic diamides: A new class of insecticides with a novel mode of action, ryanodine receptor activation. *Pestic. Biochem. Physiol. 84*, 196–214.
27. Lahm, G. P., Stevenson, T. M., Selby, T. P., Freudenberger, J. H., Cordova, D., Flexner, L., Bellin, C. A., Dubas, C. M., Smith, B. K., Hughes, K. A., Hollingshaus, J. G., Clark, C. E., and Benner, E. A. (2007) Rynaxypyr(TM): A new insecticidal anthranilic diamide that acts as a potent and selective ryanodine receptor activator. *Bioorg. Med. Chem. Lett. 17*, 6274–6279.
28. Lahm, G. P., Selby, T. P., Freudenberger, J. H., Stevenson, T. M., Myers, B. J., Seburyamo, G., Smith, B. K., Flexner, L., Clark, C. E., and Cordova, D. (2005) Insecticidal anthranilic diamides: A new class of potent ryanodine receptor activators. *Bioorg. Med. Chem. Lett. 15*, 4898–4906.
29. Zhang, Y. Z., Chen, J., Nie, Z. M., Lü, Z. B., Wang, D., Jiang, C. Y., He, P. A., Liu, L. L., Lou, Y. L., Song, L., and Wu, X. F. (2007) Expression of open reading frames in silkworm pupal cDNA library. *Appl. Biochem. Biotechnol. 136*, 327–343.
30. Hara, Y., Wakamori, M., Ishii, M., Maeno, E., Nishida, M., Yoshida, T., Yamada, H., Shimizu, S., Mori, E., Kudoh, J., Shimizu, N., Kurose, H., Okada, Y., Imoto, K., and Mori, Y. (2002) LTRPC2 Ca^{2+}-permeable channel activated by changes in redox status confers susceptibility to cell death. *Mol. Cell 9*, 163–173.
31. Miyakawa, T., Mizushima, A., Hirose, K., Yamazawa, T., Bezprozvanny, I., Kurosaki, T., and Iino, M. (2001) Ca^{2+}-sensor region of IP_3 receptor controls intracellular Ca^{2+} signaling. *EMBO J. 20*, 1674–1680.
32. Sugiyama, T., and Goldman, W. F. (1995) Measurement of SR free Ca^{2+} and Mg^{2+} in permeabilized smooth muscle cells with use of furaptra. *Am. J. Physiol. 269*, C698–C705.
33. Goonasekera, S. A., Beard, N. A., Groom, L., Kimura, T., Lyfenko, A. D., Rosenfeld, A., Marty, I., Dulhunty, A. F., and Dirksen, R. T. (2007) Triadin binding to the C-terminal luminal loop of the ryanodine receptor is important for skeletal muscle excitation−contraction coupling. *J. Gen. Physiol. 130*, 365–378.
34. Milner, R. E., Baksh, S., Shemanko, C., Carpenter, M. R., Smillie, L., Vance, J. E., Opas, M., and Michalak, M. (1991) Calreticulin, and not calsequestrin, is the major calcium binding protein of smooth muscle sarcoplasmic reticulum and liver endoplasmic reticulum. *J. Biol. Chem. 266*, 7155–7165.
35. Fraser, I. D. C., Tavalin, S. J., Lester, L. B., Langeberg, L. K., Westphal, A. M., Dean, R. A., Marrion, N. V., and Scott, J. D. (1998) A novel lipid-anchored A-kinase anchoring protein facilitates cAMP-responsive membrane events. *EMBO J. 17*, 2261–2272.
36. Yang, L., Liu, G., Zakharov, S. I., Morrow, J. P., Rybin, V. O., Steinberg, S. F., and Marx, S. O. (2005) Ser^{1928} is a common site for $Ca_v1.2$ phosphorylation by protein kinase C isoforms. *J. Biol. Chem. 280*, 207–214.

37. Fliegel, L., Burns, K., MacLennan, D. H., Reithmeier, R. A., and Michalak, M. (1989) Molecular cloning of the high affinity calcium-binding protein (calreticulin) of skeletal muscle sarcoplasmic reticulum. *J. Biol. Chem. 264*, 21522–21528.
38. Munro, S., and Pelham, H. R. B. (1987) A C-terminal signal prevents secretion of luminal ER proteins. *Cell 48*, 899–907.
39. Du, G. G., Imredy, J. P., and MacLennan, D. H. (1998) Characterization of recombinant rabbit cardiac and skeletal muscle Ca^{2+} release channels (ryanodine receptors) with a novel [^{3}H]ryanodine binding assay. *J. Biol. Chem. 273*, 33259–33266.
40. Rossi, D., Simeoni, I., Micheli, M., Bootman, M., Lipp, P., Allen, P. D., and Sorrentino, V. (2002) RyR1 and RyR3 isoforms provide distinct intracellular Ca^{2+} signals in HEK 293 cells. *J. Cell Sci. 115*, 2497–2504.
41. Querfurth, H. W., Haughey, N. J., Greenway, S. C., Yacono, P. W., Golan, D. E., and Geiger, J. D. (1998) Expression of ryanodine receptors in human embryonic kidney (HEK293) cells. *Biochem. J. 334*, 79–86.
42. Luo, D., Sun, H., Xiao, R. P., and Han, Q. (2005) Caffeine induced Ca^{2+} release and capacitative Ca^{2+} entry in human embryonic kidney (HEK293) cells. *Eur. J. Pharmacol. 509*, 109–115.
43. Kong, H., Jones, P., Koop, A., Zhang, L., Duff, H., and Chen, S. (2008) Caffeine induces Ca^{2+} release by reducing the threshold for luminal Ca^{2+} activation of the ryanodine receptor. *Biochem. J. 414*, 441–452.
44. Fill, M., and Copello, J. A. (2002) Ryanodine receptor calcium release channels. *Physiol. Rev. 82*, 893–922.
45. Mori, M. X., Erickson, M. G., and Yue, D. T. (2004) Functional stoichiometry and local enrichment of calmodulin interacting with Ca^{2+} channels. *Science 304*, 432–435.
46. Gaburjakova, M., Gaburjakova, J., Reiken, S., Huang, F., Marx, S. O., Rosemblit, N., and Marks, A. R. (2001) FKBP12 binding modulates ryanodine receptor channel gating. *J. Biol. Chem. 276*, 16931–16935.
47. Frampton, J. E., and Orchard, C. H. (1992) The effect of a calmodulin inhibitor on intracellular [Ca^{2+}] and contraction in isolated rat ventricular myocytes. *J. Physiol. 453*, 385–400.
48. Ozawa, T. (1999) Ryanodine-sensitive Ca^{2+} release mechanism of rat pancreatic acinar cells is modulated by calmodulin. *Biochim. Biophys. Acta 1452*, 254–262.
49. Wehrens, X. H., Lehnart, S. E., Reiken, S. R., and Marks, A. R. (2004) Ca^{2+}/calmodulin-dependent protein kinase II phosphorylation regulates the cardiac ryanodine receptor. *Circ. Res. 94*, e61–e70.
50. Cameron, A. M., Nucifora, F. C., Jr., Fung, E. T., Livingston, D. J., Aldape, R. A., Ross, C. A., and Snyder, S. H. (1997) FKBP12 binds the inositol 1,4,5-trisphosphate receptor at leucine-proline (1400−1401) and anchors calcineurin to this FK506-like domain. *J. Biol. Chem. 272*, 27582–27588.
51. Masumiya, H., Wang, R., Zhang, J., Xiao, B., and Chen, S. R. W. (2003) Localization of the 12.6-kDa FK506-binding protein (FKBP12.6) binding site to the NH_2-terminal domain of the cardiac Ca^{2+} release channel (ryanodine receptor). *J. Biol. Chem. 278*, 3786–3792.
52. Timerman, A. P., Ogunbumni, E., Freund, E., Wiederrecht, G., Marks, A. R., and Fleischer, S. (1993) The calcium release channel of sarcoplasmic reticulum is modulated by FK-506-binding protein. Dissociation and reconstitution of FKBP-12 to the calcium release channel of skeletal muscle sarcoplasmic reticulum. *J. Biol. Chem. 268*, 22992–22999.
53. Bultynck, G., Smet, P. D., Weidema, A. F., Heyen, M. V., Maes, K., Callewaert, G., Missiaen, L., Parys, J. B., and Smedt, H. D. (2000) Effects of the immunosuppressant FK506 on intracellular Ca^{2+} release and Ca^{2+} accumulation mechanisms. *J. Physiol. 525*, 681–693.
54. Bultynck, G., Smet, P. D., Rossi, D., Callewaert, G., Missiaen, L., Sorrentino, V., Smedt, H. D., and Parys, J. B. (2001) Characterization and mapping of the 12 kDa FK506-binding protein (FKBP12)-binding site on different isoforms of the ryanodine receptor and of the inositol 1,4,5-trisphosphate receptor. *Biochem. J. 354*, 413–422.
55. Shin, D. W., Pan, Z., Bandyopadhyay, A., Bhat, M. B., Kim, D. H., and Ma, J. (2002) Ca^{2+}-dependent interaction between FKBP12 and calcineurin regulates activity of the Ca^{2+} release channel in skeletal muscle. *Biophys. J. 83*, 2539–2549.
56. Masaki, T., Yasokawa, N., Tohnishi, M., Nishimatsu, T., Tsubata, K., Inoue, K., Motoba, K., and Hirooka, T. (2006) Flubendiamide, a novel Ca^{2+} channel modulator, reveals evidence for functional cooperation between Ca^{2+} pumps and Ca^{2+} release. *Mol. Pharmacol. 69*, 1733–1739.
57. Hamachi, I., Nagase, T., and Shinkai, S. (2000) A general semisynthetic method for fluorescent saccharide-biosensors based on a lectin. *J. Am. Chem. Soc. 122*, 12065–12066.
58. Tomohiro, T., Hashimoto, M., and Hatanaka, Y. (2005) Cross-linking chemistry and biology: Development of multifunctional photoaffinity probes. *Chem. Rec. 5*, 385–395.
59. Kiyonaka, S., Kato, K., Nishida, M., Mio, K., Numaga, T., Sawaguchi, Y., Yoshida, T., Wakamori, M., Mori, E., Numata, T., Ishii, M., Takemoto, H., Ojida, A., Watanabe, K., Uemura, A., Kurose, H., Morii, T., Kobayashi, T., Sato, Y., Sato, C., Hamachi, I., and Mori, Y. (2009) Selective and direct inhibition of TRPC3 channels underlies biological activities of a pyrazole compound. *Proc. Natl. Acad. Sci. U.S.A. 106*, 5400–5405.
60. Ponting, C., Schultz, J., and Bork, P. (1997) SPRY domains in ryanodine receptors (Ca^{2+}-release channels). *Trends Biochem. Sci. 22*, 193–194.
61. Ponting, C. P. (2000) Novel repeats in ryanodine and IP_3 receptors and protein *O*-mannosyltransferases. *Trends Biochem. Sci. 25*, 48–50.
62. Sorrentino, V., Barone, V., and Rossi, D. (2000) Intracellular Ca^{2+} release channels in evolution. *Curr. Opin. Genet. Dev. 10*, 662–667.
63. Takekura, H., Nishi, M., Noda, T., Takeshima, H., and Franzini-Armstrong, C. (1995) Abnormal junctions between surface membrane and sarcoplasmic reticulum in skeletal muscle with a mutation targeted to the ryanodine receptor. *Proc. Natl. Acad. Sci. U.S.A. 92*, 3381–3385.
64. Takeshima, H., Yamazawa, T., Ikemoto, T., Takekura, H., Nishi, M., Noda, T., and Iino, M. (1995) Ca^{2+}-induced Ca^{2+} release in myocytes from dyspedic mice lacking the type-1 ryanodine receptor. *EMBO J. 14*, 2999–3006.
65. Protasi, F., Franzini-Armstrong, C., and Allen, P. D. (1998) Role of ryanodine receptors in the assembly of calcium release units in skeletal muscle. *J. Cell Biol. 140*, 831–842.
66. Raju, B., Murphy, E., Levy, L. A., Hall, R. D., and London, R. E. (1989) A fluorescent indicator for measuring cytosolic free magnesium. *Am. J. Physiol. 256*, C540–C548.
67. Grynkiewicz, G., Poenie, M., and Tsien, R. Y. (1985) A new generation of Ca^{2+} indicators with greatly improved fluorescence properties. *J. Biol. Chem. 260*, 3440–3450.
68. Bosanac, I., Yamazaki, H., Matsu-ura, T., Michikawa, T., Mikoshiba, K., and Ikura, M. (2005) Crystal structure of the ligand binding suppressor domain of type 1 inositol 1,4,5-trisphosphate receptor. *Mol. Cell 17*, 193–203.
69. Yano, M., Yamamoto, T., Ikemoto, N., and Matsuzaki, M. (2005) Abnormal ryanodine receptor function in heart failure. *Pharmacol. Ther. 107*, 377–391.
70. Zalk, R., Lehnart, S. E., and Marks, A. R. (2007) Modulation of the ryanodine receptor and intracellular calcium. *Annu. Rev. Biochem. 76*, 367–385.
71. Dirksen, R. T., and Avila, G. (2002) Altered ryanodine receptor function in central core disease: Leaky or uncoupled Ca^{2+} release channels? *Trends Cardiovasc. Med. 12*, 189–197.
72. Ikemoto, N., and Yamamoto, T. (2000) Postulated role of interdomain interaction within the ryanodine receptor in Ca^{2+} channel regulation. *Trends Cardiovasc. Med. 10*, 310–316.
73. Orlova, E. V., Serysheva, I. I., van Heel, M., Hamilton, S. L., and Chiu, W. (1996) Two structural configurations of the skeletal muscle calcium release channel. *Nat. Struct. Biol. 3*, 547–552.
74. Sharma, M. R., Jeyakumar, L. H., Fleischer, S., and Wagenknecht, T. (2000) Three-dimensional structure of ryanodine receptor isoform three in two conformational states as visualized by cryo-electron microscopy. *J. Biol. Chem. 275*, 9485–9491.
75. Samsó, M., Trujillo, R., Gurrola, G. B., Valdivia, H. H., and Wagenknecht, T. (1999) Three-dimensional location of the imperatoxin A binding site on the ryanodine receptor. *J. Cell Biol. 146*, 493–499.
76. Tripathy, A., Resch, W., Xu, L., Valdivia, H. H., and Meissner, G. (1998) Imperatoxin A induces subconductance states in Ca^{2+} release channels (ryanodine receptors) of cardiac and skeletal muscle. *J. Gen. Physiol. 111*, 679–690.
77. Nabhani, T., Zhu, X., Simeoni, I., Sorrentino, V., Valdivia, H. H., and García, J. (2002) Imperatoxin A enhances Ca^{2+} release in developing skeletal muscle containing ryanodine receptor type 3. *Biophys. J. 82*, 1319–1328.